

Persistent oscillations of scalar and vector dispersion-managed solitons

T. I. Lakoba^{a)}

Rochester Theory Center of Optical Science and Engineering, Institute of Optics, P.O. Box 270186,
University of Rochester, Rochester, New York 14627

Dmitry E. Pelinovsky^{b)}

Department of Mathematics, University of Toronto, Toronto, Ontario, M5S 3G3 Canada

(Received 29 October 1999; accepted for publication 13 March 2000)

We show that both orthogonal and parallel internal modes exist on the background of a dispersion-managed (DM) soliton in randomly birefringent fibers. The orthogonal modes exist for arbitrarily small values of the dispersion map strength, while the parallel modes exist only when the map strength exceeds a certain threshold value. We demonstrate that initial perturbations of a DM soliton's profile that consist of one or more internal modes, exhibit nearly stable oscillations over very long propagation distances, before decaying into radiation. © 2000 American Institute of Physics. [S1054-1500(00)00303-7]

Dispersion-managed solitons are potential candidates for trans-oceanic optical telecommunication at ultrahigh bit rates. Their remarkable dynamical properties such as the ability to propagate with little distortion under the action of various perturbations over thousands of kilometers have been addressed in a great number of recent studies. In this work, we show that some part of linear dispersive radiation, which is produced when perturbations in either the transmitter or the fiber affect a dispersion-managed soliton, can be effectively trapped by a number of localized internal modes. These modes propagate along with the background soliton without visible decay over extremely long distances, manifesting their presence by small persistent oscillations of the soliton's waveform.

I. INTRODUCTION

The dispersion management technique is known to enhance the robustness of soliton pulses with respect to a number of important perturbations that occur in real-world optical telecommunication systems (see, e.g., Refs. 1 and 2). Those perturbations tend to affect the soliton parameters, such as its energy and time shift relative to the center of the bit slot, which may lead to an error when detecting the pulse at the receiving end of the system. Thus a perturbation theory which can quantify the effect of various detrimental factors on a dispersion-managed (DM) soliton, is needed. In Ref. 3, a perturbation theory based on the Hermite–Gaussian (HG) expansion for the DM soliton, was developed. The main conclusion drawn in Ref. 3 was that the variational method, based on a chirped Gaussian approximation for the DM soliton, predicts the evolution of the soliton parameters rather accurately (within 5% or so). However, perturbations not only shift the soliton parameters but also cause the soliton to emit small-amplitude radiation. This radiation can act as

noise in the transmission line, thus increasing the probability of a detection error. The perturbation theory of Ref. 3 could not be used to describe the radiation in an efficient manner, because the HG expansion is not geared for describing radiation modes, whose shape is, in general, different from the soliton shape. Among those modes, there may exist so called internal modes, which are localized in time and which are known⁴ to “trap” part of the radiation generated by a particular perturbation. That is, the radiation trapped by an internal mode escapes the vicinity of the soliton much slower than according to the conventional linear dispersive law. Therefore, if the length of the transmission line is sufficiently “short,” then the radiation trapped by the internal mode(s) does not contribute to the noise field, and the reliability of the pulse detection improves.

In this work, we demonstrate that internal modes do exist on the background of a DM soliton of both the scalar and vector DM nonlinear Schrödinger equation (NLS). The vector form of the DM NLS can be derived for averaged pulse propagation in randomly birefringent fibers by the method of Ref. 5 (see also references therein). Here we write it for the vector $\mathbf{u} = (u, v)^T$, using the notations similar to those of Ref. 3,

$$i\mathbf{u}_\xi + \frac{1}{2}D(\xi)\mathbf{u}_{tt} + \epsilon(\frac{1}{2}D_0\mathbf{u}_{tt} + G(\xi)(|u|^2 + |v|^2)\mathbf{u}) = 0. \quad (1.1)$$

The average and periodic parts, ϵD_0 and $D(\xi)$, of the dispersion coefficient, are explicitly separated in Eq. (1.1), with the average of the periodic part vanishing, $\int_0^{L_{\text{map}}} D(\xi) d\xi = 0$. The distance ξ and retarded time t are normalized so as to have $L_{\text{map}} = 1$ and $|D_1 L_1| = |D_2 L_2| = 1$, respectively. Here D_1 and D_2 are the values which the piecewise-constant coefficient $D(\xi)$ takes on in the fiber sections with respective lengths L_1 and L_2 , and $L_1 + L_2 = L_{\text{map}} (= 1)$. The coefficient $G(\xi)$ accounts for the periodic compensation of the fiber loss, with the amplification period being assumed to be an integer fraction of L_{map} . (In this way, the dispersion map sets the coarser periodicity of the system.) Parameter ϵ in Eq. (1.1) measures the size of the average-dispersion and nonlin-

^{a)}Electronic mail: lakobati@optics.rochester.edu

^{b)}Electronic mail: dmpeli@math.toronto.edu

ear terms relative to the size of the periodic-dispersion term. Explicit relations between the nondimensional parameters of Eq. (1.1), on one hand, and dimensional parameters of a real fiber and pulse, on the other, can be found, e.g., in Ref. 6.

When $\epsilon \ll 1$, Eq. (1.1) can be transformed⁷⁻⁹ into the following integro-differential form in the frequency domain,

$$i\mathbf{A}_z - \frac{1}{2}D_0\omega^2\mathbf{A} + \int \int d\omega_1 d\omega_2 \mathbf{A}(\omega_1)n(\omega, \omega_1, \omega_2) \times h((\omega_1 - \omega)(\omega_2 - \omega)) = 0, \tag{1.2}$$

where $z = \epsilon\xi$,

$$\mathbf{A}(z, \omega) \equiv \begin{pmatrix} A \\ B \end{pmatrix} = \frac{1}{2\pi} \int_0^1 d\xi \exp\left[\frac{i\omega^2}{2}\Delta(\xi)\right] \times \int dt u(\xi, t) \exp[-i\omega t], \tag{1.3}$$

$$n(\omega, \omega_1, \omega_2) = A(\omega_2)A^*(\omega_1 + \omega_2 - \omega) + B(\omega_2)B^*(\omega_1 + \omega_2 - \omega), \tag{1.4}$$

$$h(x) = \int_0^1 \exp[ix\Delta(\xi)]G(\xi)d\xi, \tag{1.5}$$

and

$$\Delta(\xi) = \Delta_0 + \int_0^\xi D(\xi')d\xi' \tag{1.6}$$

with Δ_0 arbitrary at this stage. Here and below we do not explicitly indicate the integration limits if they are infinite. Note that due to the vanishing average of $D(\xi)$, $\Delta(\xi)$ is a periodic function. Stationary solutions of the scalar versions (where one of the components identically vanishes) of Eqs. (1.1) and (1.2) were numerically found in Refs. 10 and 8, respectively.

It was first observed in numerical studies,^{11,12} and later justified by a systematic perturbation expansion,^{3,8,9,13} that in the limit $\epsilon \ll 1$, all features of a DM soliton depend on a single quantity, referred to as the map strength,

$$S \sim \frac{|D_1L_1 - D_2L_2|}{T_p^2}, \tag{1.7}$$

where T_p is a characteristic pulse width. (We do not need to specify a numerical factor in the definition of S until Sec. IV.) It can be shown that Eq. (1.1) reduces to a system of coupled NLS equations, known as the Manakov equations¹⁴ as the map strength decreases ($S \rightarrow 0$). Since the latter equations are integrable by the inverse scattering transform, they do not have internal modes in the spectrum of the linearized problem.^{15,16} However, for an arbitrary finite value of S , neither Eq. (1.1) nor (1.2) is integrable,^{17,18} and thus they may have internal modes.¹⁹ [Note: It was pointed out earlier²⁰ that Eq. (1.1) in the limit of weak dispersion management (which is equivalent to the limit $S \rightarrow 0$) is nonintegrable.] In this work, we show that internal modes do indeed exist for Eqs. (1.1) and (1.2).

This paper is organized as follows: In Sec. II, we obtain a correction to the Manakov equations that follows from Eqs. (1.1) and (1.2) in the limit of weak dispersion management

and small map strength, respectively, and show that this correction is the same in both cases. In Sec. III, we use the explicit form of this correction to show analytically that an internal mode bifurcates from the edge of the continuous spectrum of the linearized Eq. (1.1) in the limit $\epsilon \rightarrow 0$, $S \rightarrow 0$. This mode is polarized orthogonally to the background DM soliton. No copolarized internal mode exists in this limit. In Sec. IV, we proceed by solving linearized Eq. (1.2) numerically, and find a family of internal modes for a wide range of values of S . Remarkably, we find a family of copolarized internal modes, the lowest of which bifurcates from the edge of the continuous spectrum for a certain nonzero value of S . Stability of some of the lower-order modes over very long propagation distances is confirmed numerically. In Sec. V, we study the case when more than one internal modes are initially excited and show that the modes undergo slow oscillations which do not decay over distances much longer than any *trans*-oceanic distance. Finally, Sec. VI contains a summary of this work.

II. REDUCTIONS IN THE LIMIT OF WEAK DISPERSION MANAGEMENT

Here we first derive corrections to the NLS, starting from the scalar versions of Eqs. (1.1) and (1.2) in the appropriate limits, and show that the two procedures result in the same reduced model. Then we generalize this model to the vector case, thus obtaining a correction to the Manakov equations in the limit of weak dispersion management. To simplify the calculations, $G(\xi) \equiv 1$ is assumed in Secs. II and III.

The Fourier transform of Eq. (1.2) has the form⁸

$$i\mathbf{U}_z + \frac{1}{2}D_0\mathbf{U}_{tt} + \int \int dt_1 dt_2 H(t_1, t_2)\mathbf{U}(t+t_1)N(t, t_1, t_2) = 0, \tag{2.1}$$

where

$$\mathbf{U}(z, t) \equiv \begin{pmatrix} U \\ V \end{pmatrix} = \int \exp[i\omega t]\mathbf{A}(z, \omega)d\omega, \tag{2.2}$$

$$N(t, t_1, t_2) = U(t+t_2)U^*(t+t_1+t_2) + V(t+t_2)V^*(t+t_1+t_2), \tag{2.3}$$

$$H(t_1, t_2) = \frac{1}{(2\pi)^2} \int \int h(\omega_1\omega_2) \times \exp[-i\omega_1 t_1 - i\omega_2 t_2]d\omega_1 d\omega_2. \tag{2.4}$$

Let us consider reduction of system (2.1) with $V \equiv 0$ in the limit $S \rightarrow 0$. First of all, we note that S is the parameter characterizing a solution of that equation, but *not* the equation itself, because S depends on the pulse widths [cf. Eq. (1.7)]. It was shown in Refs. 8 and 9 that the main-order reduction of Eq. (2.1) in the limit $S \rightarrow 0$ coincides with the NLS. Now we derive the first-order correction to that result. In order to explicitly include the small parameter S , we perform the following scaling of variables:

$$D_0 = d_0/S, \quad t = T/\sqrt{S}, \tag{2.5}$$

with d_0 and $|U|$ being $O(1)$ quantities. Since the pulse shape and function $H(t_1, t_2)$ vary on disparate scales, T and $t \ll T$, respectively, then we can use the following formal expansion:

$$H(t_1, t_2) = S[\delta(T_1)\delta(T_2) - Sh_1\delta'(T_1)\delta'(T_2) + \frac{1}{2}S^2h_2\delta''(T_1)\delta''(T_2) + \dots], \quad (2.6)$$

where $h_1 = i\int_0^1 \Delta d\xi$ and $h_2 = -\int_0^1 \Delta^2 d\xi$. Then Eq. (2.1) becomes

$$iU_z + \frac{1}{2}d_0U_{TT} + |U|^2U = Sh_1[U_T|U|_T^2 + U(UU_T^*)_T] - \frac{1}{2}S^2h_2[U^2U_{TTTT}^* + 4UU_TU_{TTT}^* + 4U_T^2U_{TT}^* + 2U|U_{TT}|^2 + 4|U_T|^2U_{TT} + U_{TT}^2U^*]. \quad (2.7)$$

A simple asymptotic transformation,

$$U = \tilde{U} - \frac{1}{2}Sh_1\tilde{U}_{TT} + O(S^2), \quad (2.8)$$

eliminates the $O(S)$ -term in Eq. (2.7) and modifies the form of the $O(S^2)$ -term. However, we do not need to compute this modified form, because the $O(S)$ -term can also be eliminated by simply choosing the constant Δ_0 in the definition of $\Delta(\xi)$ so as to set $h_1 = 0$. This condition is just the small- S version of the condition that determines the initial chirp of a DM soliton; cf. Eq. (4.2b) below. In our nondimensional units ($|D_1L_1| = |D_2L_2| = 1$), the condition $h_1 = 0$ yields

$$\Delta_0 = -\frac{1}{2}\text{sgn}(D_1L_1), \quad (2.9)$$

and consequently, $h_2 = -1/12$. Then the following transformation:

$$U = q + \frac{S^2}{24d_0}[q_T^2q^* + 2q|q_T|^2 + q^2q_{TT}^*] + O(S^3), \quad (2.10)$$

which we found using MATHEMATICA, takes Eq. (2.7) to the form

$$iq_z + \frac{1}{2}d_0q_{TT} + f_S(|q|^2)q = 0, \quad (2.11)$$

where

$$f_S(x) = x + \frac{S^2}{24d_0}(2xx_{TT} + (x_T)^2) + O(S^3). \quad (2.12)$$

Now, Eq. (2.11) is to be compared with the equation for $\langle u \rangle = \int_0^1 u(\xi, T) d\xi$, that was derived in Ref. 21 from the scalar version of Eq. (1.1) in the limit of weak dispersion management. Here we refer to the form of this reduced equation obtained in Ref. 22. The limit of weak dispersion management corresponds to setting $D(\xi) = \epsilon d(\xi)$ in Eq. (1.1), with all the other parameters being $O(1)$ and, moreover, with $d(\xi)$, rather than $D(\xi)$, satisfying the normalization as detailed in the paragraph following Eq. (1.1). Comparing our Eqs. (2.10) and (2.11) with Eqs. (10) and (11) of Ref. 22; we see that the two sets of equations coincide, except for the term q_{TTTT} , which is missing in our Eq. (2.10). However, this term is recovered once we observe that the relation between $\langle u \rangle$ and U is given by

$$U = \langle u \rangle - \frac{1}{8}S^2h_2\langle u \rangle_{TTTT} + O(S^3), \quad (2.13)$$

whose derivation is outlined in the Appendix. Thus, Eq. (1.1) in the limit $D(\xi) = O(\epsilon)$, $\epsilon \rightarrow 0$, and Eq. (1.2) in the limit $S \rightarrow 0$, are reduced to the same model, which in the scalar case is given by Eq. (2.11). This model describes the $O(S^2)$ -correction to the NLS, that arises in the limit of weak dispersion management.

A generalization of this result to the vector case is straightforward. For example, from the vector analog of Eq. (2.1), one can obtain a system generalizing Eq. (2.7), which we do not present here because of its cumbersome form. Using MATHEMATICA, we found an asymptotic transformation,

$$\mathbf{U} = \mathbf{q} + \frac{S^2}{24d_0}[(|q|^2 + |r|^2)_T \mathbf{q}_T + (qq_T^* + rr_T^*)_T \mathbf{q}], \quad (2.14)$$

which transforms that system into a simpler form,

$$i\mathbf{q}_z + \frac{1}{2}d_0\mathbf{q}_{TT} + f_S(|q|^2 + |r|^2)\mathbf{q} = 0, \quad (2.15)$$

where $\mathbf{q} = (q, r)^T$, and the function f_S is given by (2.12).

III. INTERNAL MODES IN THE LIMIT $S \rightarrow 0$

Here we analytically establish the existence of an internal mode polarized orthogonally to the background DM soliton. Since we consider Eq. (2.15) as a small deformation of the Manakov equations, it is appropriate to reduce it to the standard form by setting $d_0 = 1$. We also introduce a small parameter,

$$\mu = \frac{S^2}{48} \ll 1, \quad (3.1)$$

to measure how far the model in question is from the integrable one.

The vector soliton of Eq. (2.15) is obtained by substituting

$$q = Q_\mu(T)e^{iz/2}, \quad r = R_\mu(T)e^{iKz/2}, \quad (3.2)$$

into that equation. Here we have used the subscript notation to indicate that the solution pertains to Eq. (2.15) with a given value of the parameter μ . For the vector generalization of the scalar DM soliton, the propagation constants of the q and r components are equal; $K = 1$, and

$$Q_\mu(T) = \cos \theta \Phi_\mu(T), \quad R_\mu(T) = \sin \theta \Phi_\mu(T), \quad (3.3)$$

where θ is an arbitrary polarization angle, and $\Phi_\mu(T)$ is the scalar DM soliton. For $\mu \ll 1$, its form is given by the asymptotic expression,²²

$$\Phi_\mu(T) = \Phi_0(T) + \mu\Phi_1(T) + O(\mu^2), \quad (3.4)$$

where $\Phi_0 = \text{sech } T$ and

$$\Phi_1 = \frac{8}{3}[2 \text{sech } T - \text{sech}^3 T - \text{sech}^5 T]. \quad (3.5)$$

To study analytically the spectrum of elementary excitations on the background of the DM soliton in the vector model, we assume the expansions,

$$q = e^{iz/2}[\Phi_\mu(T) + [\varphi_1(T) - \varphi_0(T)]e^{i\lambda z/2} + [\varphi_1^*(T) + \varphi_0^*(T)]e^{-i\lambda z/2}] \quad (3.6a)$$

and

$$r = e^{iz/2} [\psi^+(T)e^{-i\lambda z/2} + \psi^-(T)e^{i\lambda z/2}], \tag{3.6b}$$

with $|\varphi_1, \varphi_0, \psi^+, \psi^-| \ll |\Phi_\mu|$. Here we used the rotational invariance of Eq. (2.15) and thus set $\theta=0$. Linearizing Eq. (2.15), we arrive at two uncoupled linear problems,

$$\begin{aligned} \mathcal{L}_1 \varphi_1 &= \lambda \varphi_0 + 4\mu \mathcal{M}_1(T) \varphi_1, \\ \mathcal{L}_0 \varphi_0 &= \lambda \varphi_1 + 4\mu \mathcal{M}_0(T) \varphi_0, \end{aligned} \tag{3.7}$$

and

$$\mathcal{L}_0 \psi^\pm = \pm \lambda \psi^\pm + 4\mu \mathcal{M}_0(T) \psi^\pm, \tag{3.8}$$

where

$$\mathcal{L}_1 = -\partial_T^2 + 1 - 6 \operatorname{sech}^2 T, \quad \mathcal{L}_0 = -\partial_T^2 + 1 - 2 \operatorname{sech}^2 T, \tag{3.9}$$

and

$$\begin{aligned} \mathcal{M}_1(T) &= 3\Phi_0\Phi_1 + 16\Phi_0^3\Phi_{0TT} + 24\Phi_0^2\Phi_{0T}^2 \\ &\quad + 16\Phi_0^3\Phi_{0T}\partial_T + 4\Phi_0^4\partial_T^2, \end{aligned} \tag{3.10a}$$

$$\mathcal{M}_0(T) = \Phi_0\Phi_1 + 4\Phi_0^3\Phi_{0TT} + 8\Phi_0^2\Phi_{0T}^2. \tag{3.10b}$$

Linear systems (3.7) and (3.8) with $\mu=0$ occur in the analysis of perturbed Manakov equations.¹⁶ For $\mu \ll 1$, they can be analyzed by the bifurcation theory for the linearized NLS and linear Schrödinger operators, respectively.¹⁹

Linear system (3.7) describes a perturbation in the same vector component as the DM soliton. For $\mu=0$, its spectrum consists of two branches of the continuous spectrum with $|\lambda| \geq 1$ and four bound states of the discrete spectrum, all located at $\lambda=0$. These neutrally stable bound states represent infinitesimal translations of the DM soliton’s propagation constant, phase, velocity, and center. The $O(\mu)$ -term does not change the discrete spectrum but deforms the edge of the continuum at $\lambda = \pm 1$, provided that a certain bifurcation parameter κ_{par} is nonzero, where

$$\kappa_{\text{par}} = \int_{-\infty}^{\infty} dT (\varphi_{10} \mathcal{M}_1(T) \varphi_{10} + \varphi_{00} \mathcal{M}_0(T) \varphi_{00}). \tag{3.11}$$

Here $\varphi_{10} = 1 - 2 \operatorname{sech}^2 T$ and $\varphi_{00} = 1$ are the limiting eigenfunctions of the continuous spectrum for $\lambda = \pm 1$. The difference between the nondeformed and deformed edges of the continuous spectrum is that the former contains the limiting eigenvalues, along with the corresponding eigenfunctions (in this case, they are, respectively, $\lambda = \pm 1$ and $\varphi_{10}, \varphi_{00}$), whereas the latter does not contain the limiting eigenvalues and eigenfunctions, but contains those arbitrarily close to them.¹⁹ Integrable systems are known to have the edges of their continuous spectra nondeformed, while a deformed edge is an indication of nonintegrability of any given system.

Returning to Eq. (3.11), if $\kappa_{\text{par}} > 0$, then a new bound state with the eigenvalue $\lambda = \pm (1 - \mu^2 \kappa_{\text{par}}^2)$ arises from the edge of the continuum.^{19,23} If $\kappa_{\text{par}} < 0$, a new bound state does not appear. Yet, the edges of the continuum are deformed, so that points $\lambda = \pm 1$ no longer belong to it, which means that further bifurcations for nonzero but small μ are not possible.

We evaluate the integral in Eq. (3.11) using MATHEMATICA and find that

$$\kappa_{\text{par}} = -\frac{112}{15}.$$

Thus, we conclude that a nontrivial oscillatory mode does not detach from the edge of the continuum for $0 < \mu \ll 1$. Therefore, no internal mode copolarized to the background DM soliton exists for a sufficiently small map strength. Furthermore, since $\kappa_{\text{par}} \neq 0$ in this case, the $O(\mu)$ -term in Eq. (2.15) destroys integrability of the model, which coincides with the conclusion obtained earlier by different methods.^{17,18,20} A similar result was found recently for optical solitons in quadratic resonant materials.²⁴

Linear system (3.8) describes an orthogonal perturbation to the DM soliton and, in fact, reduces to two uncoupled Schrödinger problems. Since $\psi^-(T, -\lambda) = \psi^+(T, \lambda)$, in what follows we consider only the equation for ψ^+ . Its spectrum for $\mu=0$ consists of a single continuum branch with $\lambda \geq 1$ and a single bound state at $\lambda=0$. This bound state, $\psi^+ \sim \Phi_0(T)$, corresponds to a rotation of the vector DM soliton by a small angle θ . Since the $O(\mu)$ -term preserves the rotational invariance of the equation, it cannot alter this bound state. However, it does deform the edge of the continuum, provided that $\kappa_{\text{ort}} \neq 0$, where¹⁹

$$\kappa_{\text{ort}} = 2 \int_{-\infty}^{\infty} dT \psi_0^+ \mathcal{M}_0(T) \psi_0^+ \tag{3.12}$$

and $\psi_0^+(T) = \tanh T$ is the limiting eigenfunction at $\lambda=1$. Using MATHEMATICA, we find that

$$\kappa_{\text{ort}} = \frac{32}{5}.$$

Since κ_{ort} is positive, not only does the perturbation term in Eq. (2.15) deform the edge of the continuous spectrum and hence destroy integrability of the perturbed Manakov equations, but also a discrete eigenvalue $\lambda_1 = (1 - \mu^2 \kappa_{\text{ort}}^2)$ detaches from the edge point $\lambda=1$. The corresponding bound state (internal mode) $\Psi_\mu(T)$ is an odd in T , one-node solution of Eq. (3.8), whose exact form can be numerically calculated from Eqs. (3) and (4) of Ref. 19.

Let us now briefly discuss the role of this new internal mode. First, as pointed out in Sec. 1, it can trap some part of radiation polarized orthogonally to the DM soliton, so that this radiation would remain in the vicinity of the soliton over a much longer distance than it would if the internal mode were absent. Second, we conjecture that a superposition of a scalar DM soliton and the orthogonally polarized internal mode, which has the form (3.2) with $\mathcal{K} = \mu^2 \kappa_{\text{ort}}^2$ and

$$Q_\mu = \Phi_\mu(T) + O(\nu^2), \quad R_\mu = \nu \Psi_\mu(T) + O(\nu^3), \tag{3.13}$$

where $\nu \ll 1$, is a member of a new family of asymmetric vector solitons of Eqs. (1.1) or (1.2). A numerical proof of existence of such family of asymmetric solitons would require having a fast algorithm of finding stationary solitons of Eq. (1.2), which we do not have at the moment. We postpone further qualitative discussion of this issue until Sec. V.

IV. INTERNAL MODES FOR ARBITRARY MAP STRENGTH

For arbitrary values of the map strength, it is more convenient to consider equations written in the frequency domain, and then transform the solution back into the time domain by inverting Eq. (1.3). Thus, below we numerically determine internal modes of Eq. (1.2), linearized on the background of a DM soliton.

First of all, owing to the rotational invariance of these equations, we are free to take the background soliton being polarized along the *A*-component. Then the linearized problem splits into two uncoupled ones, which are counterparts of Eqs. (3.7) and (3.8). Next, since we could not efficiently determine the exact shape of a stationary scalar DM soliton, we have to approximate it by a Gaussian. In selected cases, we verified that including corrections that arise due to the next Hermite–Gaussian component in the expansion of the DM soliton shape,^{3,25} changed our results only slightly.

Without loss of generality, we set the maximum amplitude (measured in the time domain) of the Gaussian to unity. In the frequency domain, the corresponding approximate shape of the DM soliton is (see, e.g., Ref. 6)

$$A_0(z, \omega) = \frac{T_0}{\sqrt{2\pi}} \exp\left[-\frac{1}{2}(\omega T_0)^2 + ik_{\text{sol}}z\right] \equiv A_0(\omega) \exp[ik_{\text{sol}}z]. \quad (4.1)$$

Here T_0 is the minimum width of the Gaussian in the time domain, which is related to the average dispersion D_0 by the following equation (see Refs. 3, 2, and references therein):

$$D_0 = T_0^2 \text{Re } I_2 / \sqrt{2}, \quad (4.2a)$$

where I_2 is obtained from

$$I_n = \int_0^1 \left(\frac{1+i\Delta/T_0^2}{1-i\Delta/T_0^2}\right)^{n/2} \frac{G(\xi)d\xi}{\sqrt{1+\Delta^2/T_0^4}}, \quad n=0,1,\dots \quad (4.3)$$

Integrals I_n appear in expansion of a DM soliton over the basis of Hermite–Gaussian functions.³ We remind the reader that we use the normalization of the time variable such that $|D_1 L_1| = |D_2 L_2| = 1$ (cf. Sec. I). The values of I_n depend on the initial constant Δ_0 [cf. Eq. (1.6)], which is found from the equation

$$\text{Im } I_2 = 0. \quad (4.2b)$$

The soliton propagation constant, k_{sol} , is related to T_0 by³

$$k_{\text{sol}} = (1/\sqrt{2})(I_0 - I_2/4). \quad (4.4)$$

For a lossless fiber, where $G(\xi) = 1$, all integrals I_n can be evaluated explicitly. Then, Eq. (4.2b) yields the value for Δ_0 as given by Eq. (2.9), and Eqs. (4.2a) and (4.4) become

$$D_0 = \sqrt{2} T_0^4 \left[\frac{2}{(1+4T_0^4)^{1/2}} - \ln\left(\frac{1+(1+4T_0^4)^{1/2}}{2T_0^2}\right) \right]$$

and

$$k_{\text{sol}} = \frac{T_0^2}{2\sqrt{2}} \left[-\frac{2}{(1+4T_0^4)^{1/2}} + 5 \ln\left(\frac{1+(1+4T_0^4)^{1/2}}{2T_0^2}\right) \right].$$

Equations (4.1)–(4.4) illustrate the fact, mentioned in Sec. I, that the only parameter of the family of scalar DM solitons is T_0 , or, equivalently, the map strength, which we define here as

$$S = 1/(2T_0^2). \quad (4.5)$$

This quantity is by a factor of $\ln 2$ smaller⁶ than the map strength originally introduced in Ref. 11. Thus, in what follows we consider both D_0 and k_{sol} as functions of S , and also parametrize the family of internal modes by this quantity.

A. Orthogonal internal modes

The linearization of Eq. (1.2) for the orthogonal internal mode $b(\omega)$ reads

$$\left(k_{\text{sol}} - \lambda + \frac{D_0}{2}\omega^2\right)b(\omega) = \int d\omega' b(\omega') K^{(1)}(\omega', \omega), \quad (4.6)$$

where $B(z, \omega) = b(\omega) \exp[i(k_{\text{sol}} - \lambda)z]$ and

$$K^{(1)}(\omega', \omega) = \int d\omega'' A_0(\omega'') A_0^*(\omega' + \omega'' - \omega) \times h[(\omega' - \omega)(\omega'' - \omega)]. \quad (4.7)$$

An eigenvalue $\lambda = k_{\text{node}}$ is that of an internal mode, provided that the function $v(z, t)$, found from the corresponding eigenfunction $b(\omega)$, is localized in t . For other values of λ , $v(z, t)$ oscillates with t as $|t| \rightarrow \infty$.

The stationary DM soliton is an even function of t , hence $A_0(\omega) = A_0(-\omega)$ and the kernel $K^{(1)}(\omega', \omega)$ has a symmetry

$$K^{(1)}(\omega', \omega) = K^{(1)}(-\omega', -\omega). \quad (4.8)$$

Another symmetry of $K^{(1)}(\omega', \omega)$ follows from the relation $h(-x) = h^*(x)$, using which one obtains

$$K^{(1)}(\omega', \omega) = K^{(1)*}(\omega, \omega'). \quad (4.9)$$

This means that the Fredholm equation (4.6) is self-adjoint, and its eigenvalues are all real. Symmetry (4.8) means that $b(\omega)$ and $b(-\omega)$ satisfy the same equation, and therefore one can look for even and odd internal modes separately. This circumstance is used to reduce the computational time of solving Eq. (4.6) numerically, since for a mode with a certain parity, this equation can be rewritten as

$$\left(k_{\text{sol}} - \lambda + \frac{D_0}{2}\omega^2\right)b_{o,e}(\omega) = \int_0^\infty d\omega' b_{o,e}(\omega') K_{o,e}^{(1)}(\omega', \omega), \quad (4.10)$$

where $\omega > 0$ and

$$K_{o,e}^{(1)}(\omega', \omega) = K^{(1)}(\omega', \omega) \mp K^{(1)}(\omega', -\omega). \quad (4.11)$$

The label ‘‘o’’ (‘‘e’’) pertains to odd (even) modes. Equation (4.10) is solved by replacing the integral by a finite sum (see, e.g., Ref. 26) that extends over the set $\{\omega'_n = (n-1)\delta\omega\}_{n=1}^{n_{\text{max}}}$ for some $\delta\omega$ and n_{max} . The discrete vector $\hat{\mathbf{b}}_{o,e} = \{b(\omega_n)\}_{n=1}^{n_{\text{max}}}$ is a solution of a linear algebraic eigenvalue problem,

TABLE I. Orthogonal internal modes.

Map strength, S	$(k_{\text{mode}})_o/k_{\text{sol}}$	$(k_{\text{mode}})_e/k_{\text{sol}}$
0.1	0.998	
0.25	0.995	
0.5	0.976	
0.75	0.931	
1.0	0.873	
1.5	0.745	0.979
2.0	0.644, 0.969	0.861
2.5	0.572, 0.849, 0.969	0.748, 0.918
3.0	0.519, 0.734	0.659, 0.786
	+5 more modes	+5 more modes
3.28 ($\approx S_{\text{cr}}$)	0.496	0.617
	$+\infty$ more (?)	$+\infty$ more (?)
3.5 ^a	0.479	0.687
4.0 ^a	0.448	
4.5 ^a	0.418	

^aFor $S > S_{\text{cr}}$, modes are quasilocalized. Eigenvalues of only the first one or two such modes are listed.

$$\left(k_{\text{sol}} + \frac{D_0}{2} \hat{\omega}^2 - \delta\omega \hat{K}_{o,e}^{(1)} W \right) \hat{\mathbf{b}}_{o,e} = \lambda \hat{\mathbf{b}}_{o,e}, \quad (4.12)$$

where $(\hat{K}_{o,e}^{(1)})_{mn} = K_{o,e}^{(1)}(\omega'_m, \omega_n)$ and $\hat{\omega}^2 = \text{diag}(\omega_1^2, \omega_2^2, \dots, \omega_{n_{\text{max}}}^2)$. The weight matrix W depends on the approximation by which the integral is converted into a finite sum, e.g., when the Simpson rule is used, $W = \text{diag}(1/3, 4/3, 2/3, 4/3, \dots, 2/3, 4/3, 1/3)$. System (4.12) can be solved using any computer linear algebra package. Let us note that the matrix elements $(\hat{K}_{o,e}^{(1)})_{mn}$ can be efficiently evaluated by any standard numerical integration routine using the known analytical expressions for $h(\omega_1, \omega_2)$ and $A_0(\omega)$.

Before presenting the results of numerical solution of Eq. (4.12), let us discuss what its spectrum is expected to look like. As noted above, this spectrum is purely real. Moreover, $\lambda = 0$ is always an eigenvalue, corresponding to the rotational invariance of the DM soliton. If we now assume that the inverse Fourier transform of the integral term in Eq. (4.6) vanishes faster than the linear one for $|t| \rightarrow \infty$, as is the case for Eq. (3.8), then, for $D_0 > 0$, the continuous and possible discrete eigenvalues occupy the regions $\lambda > k_{\text{sol}}$ and $0 < \lambda < k_{\text{sol}}$, respectively. Any internal mode is to detach from the edge point $\lambda = k_{\text{sol}}$ of the continuous spectrum. Now, to our knowledge, the above assumption about the asymptotic behavior of the integral term in Eq. (4.6) or its Fourier transform has not been rigorously proven. Nonetheless, the results we find for $D_0 > 0$ are as predicted above. For $D_0 < 0$, the situation is not so obvious, and it will be clarified as we proceed. Finally, let us mention that the Fourier transforms of the odd and even solutions $b_{o,e}$ are counterparts of the following solutions of the linear Schrödinger equation (3.8) with $\mu = 0$; $\exp[ikT](-ik + \tanh T) \mp \exp[-ikT](ik + \tanh T)$, respectively, where $k = \sqrt{\lambda - 1}$.

The normalized eigenvalues of odd (“o”) and even (“e”) internal modes, obtained by numerically solving Eq. (4.12) with $\delta\omega = 2\pi/(MT_0)$ and $n_{\text{max}} = 81$, are presented in Table I. We use $M = 100$ for all values of S , except for $S = 0.1$, for which we have to use a wider interval in time (with $M = 120$), because for small S , the internal mode is very

weakly localized. The critical value of the map strength corresponding to $D_0 = 0$ is $S_{\text{cr}} \approx 3.28$. For $S \geq S_{\text{cr}}$, we also increase n_{max} to verify the asymptotic behavior of the internal modes. All the calculations are performed for the lossless fiber [$G(\xi) = 1$], but exactly the same procedure can be used, and qualitatively the same results are expected, when the fiber is periodically amplified. We verify that there always exists an even eigenfunction with $\lambda \approx 0$; deviations from the exact zero, for which we always found $\lambda/k_{\text{sol}} < 7\%$, are attributed to the fact that the background solution was not an exact DM soliton. It is also interesting to note that for $S > 1$, the neutral mode with $\lambda \approx 0$ has “wings” very similar to those of a stationary DM soliton (see, e.g., Refs. 12, 10). That is, this neutral mode, whose shape must be exactly that of a stationary DM soliton, “tries” to be of the proper shape even though the background solution is not.

For $D_0 > 0$, we find the eigenvalues of internal modes by looking for them in the interval $(0, k_{\text{sol}})$, as explained above. The number of the internal modes increases as S approaches the critical value, S_{cr} , where the average dispersion changes sign. For a given $S < S_{\text{cr}}$, the number of oscillations in the profile of an internal mode increases with the mode’s number. Also, the eigenvalues of internal modes are seen to occupy only the upper half, $(k_{\text{sol}}/2, k_{\text{sol}})$, of the allowed interval. For $S = 3.28$ (corresponding to the exact value $D_0 = 3.16 \times 10^{-4}$), the number of internal modes found strongly depends on n_{max} . For $n_{\text{max}} = 81$, we find 19 odd and 19 even localized modes, while for $n_{\text{max}} = 241$, the number of each type of modes increases to 26. With our numerical resolution (10^{-16}), we cannot see any oscillating tails; all the 26 modes are localized. Therefore, we think that for $S = S_{\text{cr}}$, an infinite number of internal modes exist. For $D_0 < 0$, all the eigenvalues occupy the region $(-\infty, k_{\text{sol}})$, and the interval $(0, k_{\text{sol}})$ contains eigenvalues pertaining to both localized and nonlocalized modes. In that case, we first take n_{max} sufficiently small ($n_{\text{max}} = 81$) and visually examine all of the eigenmodes, whose eigenvalues are in that interval; those localized are the internal modes. Next, we increase n_{max} to 509 and verify that these modes remain either localized or quasilocalized (i.e., develop very small oscillating tails extending to infinity). In fact, we find that all of the internal modes do become quasilocalized for $D_0 < 0$, whereas the neutral mode with $\lambda \approx 0$ remains localized even then, at least within our numerical resolution. Thus, the internal modes do not exist for $D_0 < 0$ in the strict sense. Nonetheless, for the reasons that we explain shortly, we still list the eigenvalues of a few lowest quasilocalized modes.

As it was explained in Sec. I, the main role played by internal modes in the dynamics of a soliton is that they trap part of radiation and force it to remain in the soliton’s vicinity over a very long distance. In particular, if a perturbation of the soliton’s profile initially coincides with an internal mode, then this perturbation preserves its shape over a long distance. This is illustrated in Figs. 1–3, which are obtained by numerically solving Eq. (1.1) with $\epsilon = 0.2$ and $G(\xi) = 1$ over 600 map periods. Figure 1 shows, for $S = 1.5$, evolutions of the odd internal mode [Fig. 1(a)] and a perturbation [Fig. 1(b)] whose profile at the chirp-free point of the map is

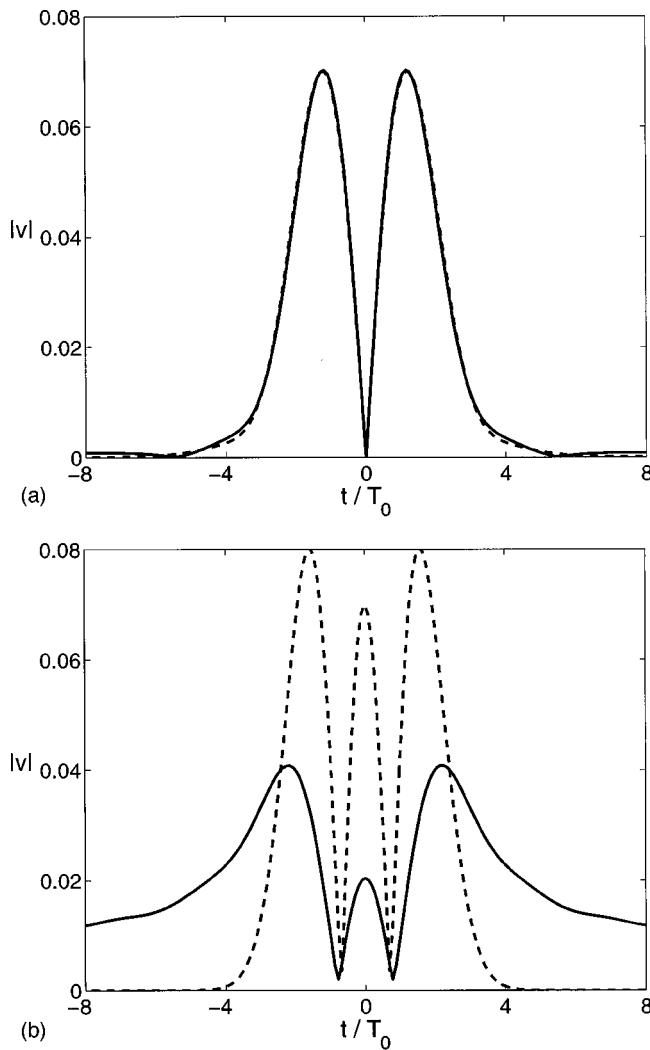


FIG. 1. Evolutions of the orthogonal odd internal mode (a) and perturbation (4.13) for $S=1.5$. Solid, profile at $\xi=600L_{\text{map}}$; dashed, initial profile.

$$v \propto (1 - 2t^2/T_0^2) \exp[-t^2/(2T_0^2)]. \quad (4.13)$$

Perturbation (4.13) is orthogonal to both the odd internal mode and the Gaussian approximation of the neutral mode. (Here orthogonality is used in the sense of a functional inner product as in, e.g., Ref. 16, rather than in the sense of polarization.) It is also approximately orthogonal to the even internal mode (cf. Table I), because the latter is only weakly localized (its eigenvalue lies close to the edge of the continuous spectrum). Thus, perturbation (4.13) consists mostly of the continuous spectrum eigenfunctions, and is seen to considerably spread out over 600 map periods, while the internal mode remains almost unchanged over the same distance. Figures 2(a) and 2(b) show similar evolutions, but for $S=3$. In this case, a significant part of perturbation (4.13) is found in the first *even* internal mode [compare Figs. 2(b) and 2(c)], and therefore it decays much less than in Fig. 1(b). Finally, Figs. 3(a) and 3(b) show evolutions of, respectively, a localized initial perturbation, which was obtained by “cutting off” the oscillating tails of the quasilocalized odd mode for $S=4.5$, and a perturbation of the form (4.13) for the same value of S . This value was chosen sufficiently “far” into the

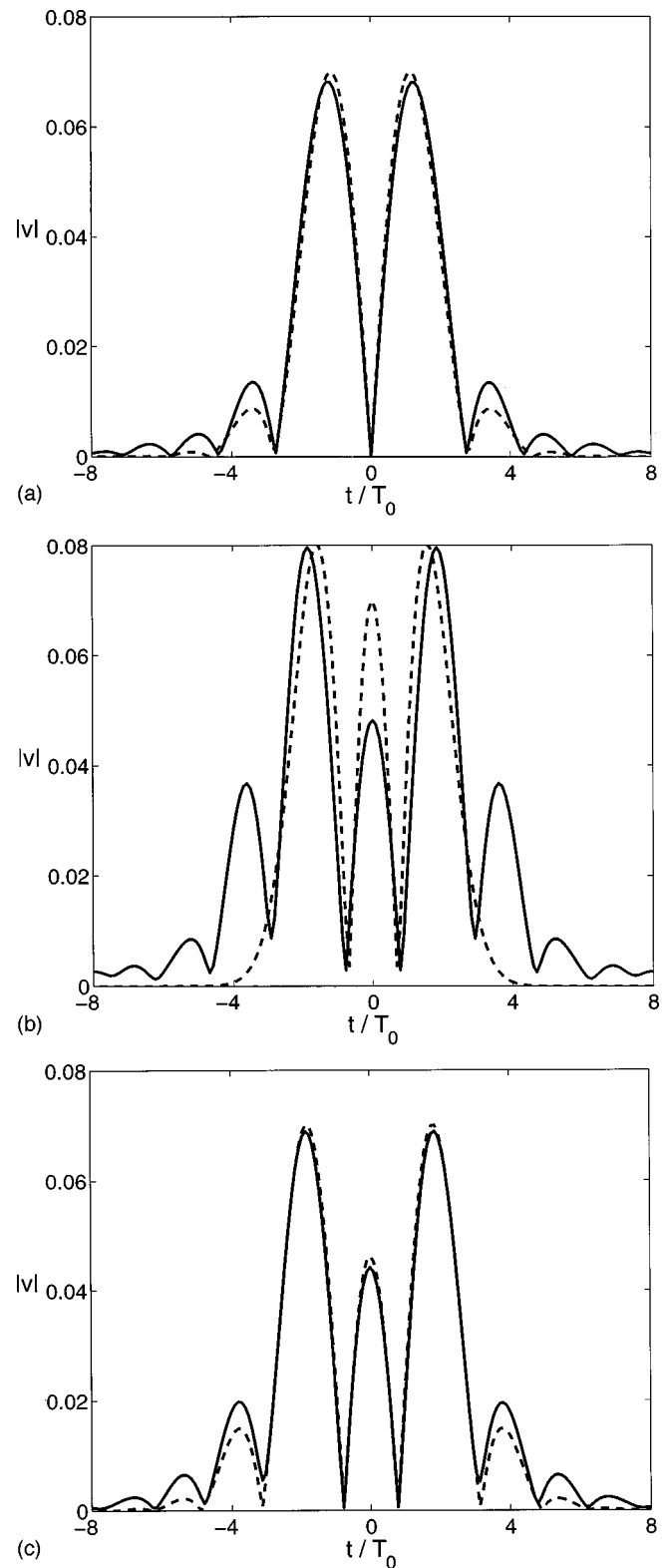


FIG. 2. Evolutions of the lowest orthogonal odd (a) and even (c) internal modes and perturbation (4.13) (b) for $S=3.0$. Solid, profile at $\xi=600L_{\text{map}}$; dashed, initial profile.

region where $D_0 < 0$, so as to ensure that only one quasilocalized mode has tails whose amplitude is much less than that of the mode’s central part. That is, all the other modes are indistinguishable from the modes of the continuous spectrum. Figure 3 clearly shows that a perturbation that is ini-

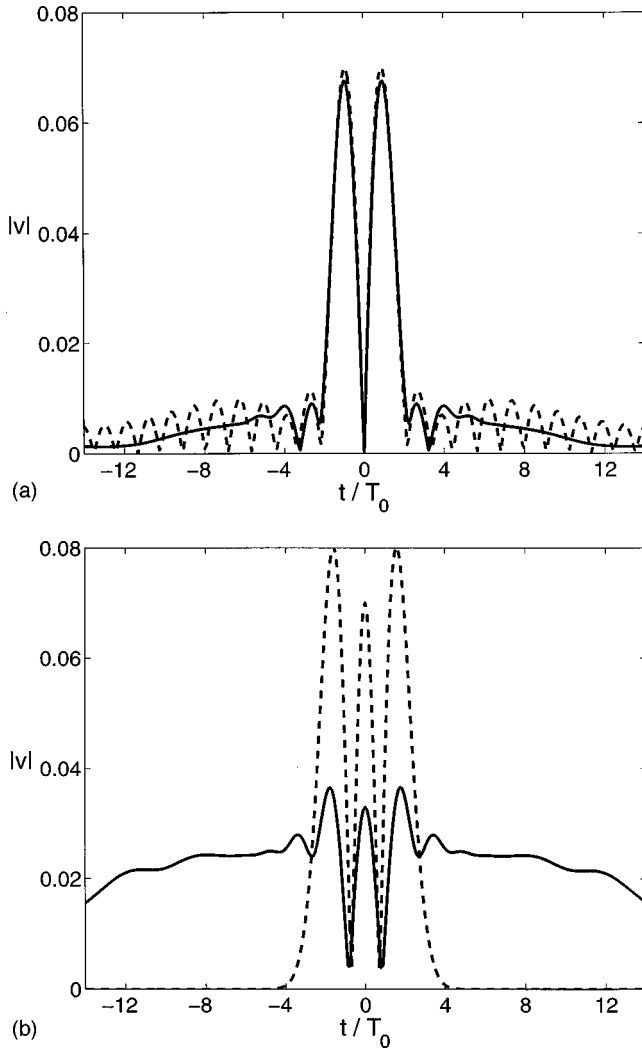


FIG. 3. Evolutions of the orthogonal odd quasi-localized mode (a) and perturbation (4.13) (b) for $S=4.5$. Solid, profile at $\xi=600L_{\text{map}}$; dashed, initial profile.

tially close to even a quasilocalized mode decays at a much slower rate than a perturbation consisting of an arbitrary combination of the continuous spectrum modes. Thus, quasilocalized modes can play similar part in the dynamics of a DM soliton for $D_0 < 0$ as true internal modes play for $D_0 > 0$.

B. Parallel internal modes

The procedure of finding internal modes parallel to the DM soliton is similar to that described above. Substituting $A = (A_0 + a)\exp[ik_{\text{sol}}z]$, $B = 0$, $|a| \ll |A_0|$ into Eq. (1.2) and linearizing, one obtains the following equation for the vector $\mathbf{a} = (a, a^*)^T \exp[-i\lambda z]$:

$$\lambda \mathbf{a}(\omega) = -\sigma_3 \left(k_{\text{sol}} + \frac{D_0}{2} \omega^2 \right) \mathbf{a}(\omega) + \int (2\sigma_3 K^{(1)}(\omega', \omega) + i\sigma_2 K^{(2)}(\omega', \omega)) \mathbf{a}(\omega') d\omega', \quad (4.14)$$

where

$$K^{(2)}(\omega', \omega) = \int d\omega'' A_0(\omega'') A_0(\omega' - \omega'' + \omega) \times h^*[(\omega' - \omega'')(\omega - \omega'')], \quad (4.15)$$

and

$$\sigma_1 = \begin{pmatrix} 0 & 1 \\ 1 & 0 \end{pmatrix}, \quad \sigma_2 = \begin{pmatrix} 0 & -i \\ i & 0 \end{pmatrix}, \quad \sigma_3 = \begin{pmatrix} 1 & 0 \\ 0 & -1 \end{pmatrix}$$

are the Pauli matrices (matrix σ_1 is referred to later on). Kernel $K^{(2)}$ has the following symmetries:

$$K^{(2)}(\omega', \omega) = K^{(2)}(-\omega', -\omega), \quad (4.16)$$

$$K^{(2)}(\omega', \omega) = K^{(2)}(\omega, \omega'). \quad (4.17)$$

Symmetry (4.16) means that even and odd eigenmodes can be considered separately. They are counterparts of the following eigenfunctions of the linearized NLS: $\psi(T, k) \pm \psi(-T, -k) + \psi(T, -k) \pm \psi(-T, k)$.²⁷ Symmetry (4.17) has no obvious consequences. Replacing the integral term in Eq. (4.14) by a discrete sum, we obtain for the vector

$$\hat{\mathbf{a}} = (a(\omega_1), \dots, a(\omega_{n_{\text{max}}}), a^*(\omega_1), \dots, a^*(\omega_{n_{\text{max}}})) \times \exp[-i\lambda z],$$

the following linear algebraic equation:

$$\lambda \hat{\mathbf{a}} = - \left\{ \text{diag} \left[k_{\text{sol}} + \frac{D_0}{2} \hat{\omega}^2, - \left(k_{\text{sol}} + \frac{D_0}{2} \hat{\omega}^2 \right) \right] \right\} \hat{\mathbf{a}} + \begin{pmatrix} 2\hat{K}^{(1)}W & \hat{K}^{(2)}W \\ -\hat{K}^{(2)}W & -2\hat{K}^{(1)}W \end{pmatrix} \hat{\mathbf{a}}. \quad (4.18)$$

Matrix $\hat{K}^{(2)}$ is defined similar to $\hat{K}^{(1)}$ and is symmetric [see (4.17)], whereas $\hat{K}^{(1)}$ is Hermitian. As a collateral remark, serving to make comparison with the linearized NLS,²⁷ we note that the solution $\hat{\mathbf{a}}_{\text{adj}}$ of an equation adjoint to (4.18) is related to the solution of Eq. (4.18) by

$$\hat{a}_{\text{adj}} = \hat{\sigma}_3 \hat{a}^*, \quad \hat{\sigma}_3 = \text{diag}(\underbrace{1, 1, \dots, 1}_{n_{\text{max}}}, \underbrace{-1, -1, \dots, -1}_{n_{\text{max}}}), \quad (4.19)$$

only if $\hat{K}^{(2)}$ is also Hermitian. This can only be so when all the elements of this matrix are real, which occurs, for example, in the case of a lossless fiber, where $h(x) = \sin(x/2)/(x/2)$. In the NLS limit (i.e., $S \rightarrow 0$), $K^{(2)}$ is also real, even for a periodically amplified fiber.

Since the eigenvalue problem (4.18) is not Hermitian, its spectrum cannot be guaranteed to be real *a priori*. However, in all our numerical simulations, we found that it is indeed real, except for the eigenvalues corresponding to the two lowest odd eigenmodes. If the exact stationary DM soliton is substituted for A_0 in Eq. (4.16) or (4.18), these equations have four neutral modes with the same eigenvalue $\lambda = 0$ (cf. Sec. III). However, since in our procedure, A_0 is not the exact DM soliton, this fourfold degenerate eigenvalue splits into four simple eigenvalues located around zero ($|\lambda| < 0.1k_{\text{sol}}$). Two of them, corresponding to the even neutral modes, remain real, while the other two, corresponding to the odd eigenmodes, become imaginary. A similar fact regarding the latter eigenmodes was earlier noted in (Ref. 3).

TABLE II. Parallel internal modes.

Map strength, S	$(k_{\text{mode}})_e/k_{\text{sol}}$	$(k_{\text{mode}})_o/k_{\text{sol}}$
0.7	0.995	
1.0	0.917	
1.5	0.675	0.935
2.0	0.472, 0.867	0.699, 0.971
2.5	0.335, 0.652	0.511, 0.755
3.0	+2 more modes	+2 more modes
	0.244, 0.484	0.379, 0.560
	+8 more modes	+7 more modes
3.28	0.207, 0.409	0.323, 0.469
	$+\infty$ more (?)	$+\infty$ more (?)
3.5 ^a	0.182	0.285
4.0 ^a	0.137	0.215

^aSee footnote in Table I.

For $D_0 > 0$ the continuous spectrum occupies the branches $(-\infty, -k_{\text{sol}}]$ and $[k_{\text{sol}}, \infty)$, and thus any localized modes may only be found inside the interval $(-k_{\text{sol}}, k_{\text{sol}})$. For $D_0 < 0$, the two branches of the continuous spectrum intersect over this interval, and therefore the localized modes can only be found by visual examination, as explained earlier for orthogonal eigenmodes. Our numerical results are summarized in Table II. Since the eigenvalues always come in pairs as $\pm\lambda$,²⁷ we only list the positive eigenvalue. The corresponding eigenfunctions are related by $\mathbf{a}(-\lambda) = \sigma_1 \mathbf{a}^*(\lambda)$.²⁷ Note that in contrast to the case of orthogonal internal modes, the first parallel internal mode that detaches from the edge of the continuum is even in t (or ω). Similar to the case of orthogonal modes, there appear to be an infinite number of internal modes for $S = S_{\text{cr}}$, while these modes become quasilocalized for $S > S_{\text{cr}}$.

Numerical verification of long-term stability of parallel internal modes is somewhat more involved than that of orthogonal modes. The Gaussian approximation for the DM soliton, which we have to use, is a superposition of the *exact* DM soliton and some combination of internal modes with small amplitudes. These modes evolve each with its own propagation constant, thus making extraction of the desired one mode not a straightforward task. Furthermore, the approximately determined internal mode contains a small component of the exact neutral mode. The latter, when added to the background soliton, leads to linear increase of its overall phase, which becomes appreciable over long distances. Thus, to compare the initial and final mode profiles, the component arising due to the slow accumulation of the soliton's phase should always be subtracted. Now, if $\mathbf{a} \equiv (a^{(1)}, a^{(2)})^T$ is any eigenfunction of Eq. (4.14), then the corresponding initial condition for the scalar quantity a is $(c + id)a^{(1)} + (c - id)a^{(2)*}$, where c and d are real constants.²⁷ For the case of a lossless fiber, the components $a^{(1,2)}$ of an internal mode can always be taken to be real. Then the evolution of such a perturbation is [compare with Eq. (3.6a)]

$$\begin{aligned}
 a = & c[a(a^{(1)} + a^{(2)})\cos(\lambda z) + i(a^{(1)} - a^{(2)})\sin(\lambda z)] \\
 & + d[i(a^{(1)} - a^{(2)})\cos(\lambda z) + (a^{(1)} + a^{(2)})\sin(\lambda z)],
 \end{aligned}
 \tag{4.20}$$

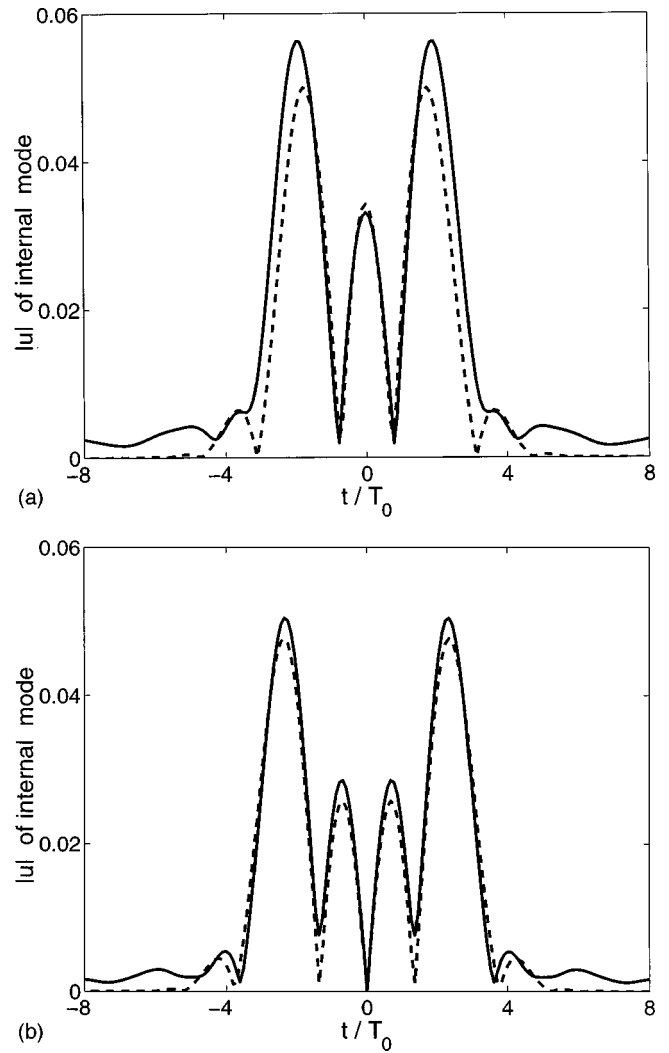


FIG. 4. Evolutions of the lowest even (a) and odd (b) parallel internal modes over $\xi = 1000L_{\text{map}}$ ($\epsilon = 0.1$) for $S = 2.0$. Solid, profile at $\xi = 1000L_{\text{map}}$; dashed, initial profile.

where λ is the corresponding eigenvalue. Then, calculating *separately* evolutions of two initial perturbations, one with $c = 0$ and the other with $d = 0$, one can obtain profiles of both $a^{(1)} \pm a^{(2)}$ for arbitrarily long distances of propagation. The results obtained in this way for evolution of an initial perturbation corresponding to $a^{(1)} + a^{(2)}$ and for $S = 2.0$ are shown in Fig. 4. Note that if one only calculates evolution of just one of the above perturbations (with *either* $c = 0$ or $d = 0$) and then attempts to use the known values of $\cos(\lambda z)$ and $\sin(\lambda z)$ to extract $a^{(1)} \pm a^{(2)}$, one may fail to achieve that if z is sufficiently large, because of limited accuracy (some few percent) with which the eigenvalues are determined.

V. SIMULTANEOUS EXCITATION OF SEVERAL INTERNAL MODES

Here we study nonlinear dynamics of small orthogonal perturbations to the DM soliton. A generic perturbation is a superposition of localized modes, both neutral and internal, and modes of the continuous spectrum. The latter decay as $O(z^{-1/2})$ and thus can be neglected in comparison with the long-living localized modes. In other words, after the con-

tinuous spectrum component is “washed out” over a distance $O(\epsilon^{-2})$, there is left a “skeleton” of the initial perturbation, consisting only of the localized modes. The motivation for studying nonlinear interaction of these modes is provided by the results of a recent paper,²⁸ where such interaction was considered for the case of solitons in a constant-birefringence fiber. The authors of Ref. 28 showed that the lower-order internal modes, orthogonal to the background scalar soliton, may suppress higher-order ones by causing them to decay into continuum radiation exponentially fast. Thus, in the case considered in Ref. 28, only the lowest-order localized mode from the initial perturbation would survive and form, together with the background scalar soliton, a new vector soliton. The main result obtained in this section is that in the case of a DM soliton of Eq. (1.1), the nonlinear interaction among the localized modes does not lead to suppression of any of them, at least on the length scale considered in Ref. 28. Instead, the modes undergo oscillations that do not decay visibly over a few thousand map periods, which by far exceeds the length of any *trans*-oceanic fiber link.

We consider the simplest case where the initial perturbation consists of only two orthogonal modes, and further restrict our analysis to the limit of small S , where fully analytical treatment is possible. For a finite nonzero value of the map strength, similar considerations can be shown to give qualitatively the same results. For $S \ll 1$, the model is described by Eq. (2.15), in which we use the same normalization, $d_0 = 1$ and $\mu = S^2/48$ as in Sec. III. The orthogonal perturbation to the DM soliton (3.3) with $\theta = 0$ has the form given by Eqs. (3.2) and (3.13), with ν being a small parameter measuring the size of the orthogonal component. Using an asymptotic multiscale method, we extend this form to higher orders in ν as follows:

$$q = e^{iz/2} [Q_0(T) + \nu^2 Q_2(z, T) + O(\nu^4)], \tag{5.1}$$

$$r = \nu R_1(z, T) + \nu^3 R_3(z, T) + O(\nu^5), \tag{5.2}$$

where $Q_0 = \Phi_\mu(T)$ and

$$R_1 = c_1(z_2) \Phi_\mu(T) e^{iz/2} + c_2(z_2) \Psi_\mu(T) e^{ik_\mu z/2}. \tag{5.3}$$

The first term in Eq. (5.3) is the neutral mode and the second one is the internal mode. They have even and odd parity in T , respectively. The parameter $k_\mu = \mu^2 \kappa_{\text{ort}}^2$ (cf. end of Sec. III) is the propagation constant of the internal mode, and the amplitudes c_1 and c_2 are constant on the scale z but may evolve on the slower scale, $z_2 = \nu^2 z$.

The correction term $Q_2(z, T)$ to q is induced by a term that is quadratic in the orthogonal perturbation r ,

$$\begin{aligned} Q_2 = & |c_1|^2 w_1(T) + |c_2|^2 w_2(T) \\ & + c_1 c_2^* (w_3(T) - w_4(T)) e^{i(1-k_\mu)z/2} \\ & + c_1^* c_2 (w_3^*(T) + w_4^*(T)) e^{-i(1-k_\mu)z/2}. \end{aligned} \tag{5.4}$$

Here $w_1(T)$ to $w_4(T)$ solve the equations

$$\mathcal{L}_1 w_1 = 4\mu \mathcal{M}_1 w_1 + \Phi_\mu f'_S [\Phi_\mu^2] (\Phi_\mu^2), \tag{5.5}$$

$$\mathcal{L}_1 w_2 = 4\mu \mathcal{M}_1 w_2 + \Phi_\mu f'_S [\Phi_\mu^2] (\Psi_\mu^2), \tag{5.6}$$

$$\mathcal{L}_1 w_3 = (1 - \omega_\mu) w_4 + 4\mu \mathcal{M}_1 w_3 + \Phi_\mu f'_S [\Phi_\mu^2] (\Phi_\mu \Psi_\mu), \tag{5.7}$$

$$\mathcal{L}_0 w_4 = (1 - \omega_\mu) w_3 + 4\mu \mathcal{M}_0 w_4, \tag{5.8}$$

where operators $\mathcal{L}_1, \mathcal{L}_0$ and functions $\mathcal{M}_1, \mathcal{M}_0$ are defined in Eqs. (3.9) and (3.10), and $f'_S[x](y)$ is the Fresnet derivative of the operator function $f_S(x)$. Now, since the vector soliton (3.3) is an exact solution of Eqs. (2.15), we find an exact solution of Eq. (5.5) as $w_1 = -\frac{1}{2} \Phi_\mu(T)$. The correction term $w_2(T)$ represents the second-order correction to the asymmetric soliton in the asymptotic expansion (3.4). The z -dependent terms in Q_2 are shown below to lead to interaction and oscillatory dynamics of the two orthogonal modes. Since the eigenvalue $\lambda = 1 - k_\mu$ lies in the gap of the continuous spectrum of the linear eigenvalue problem (3.7), the functions $w_3(x)$ and $w_4(x)$ are real and localized in T . Thus, no radiation occurs at the order $O(\nu^2)$ of the asymptotic expansion.

The correction term $R_3(z, T)$ has the following form:

$$\begin{aligned} R_3 = & v_1(z_2, T) e^{iz/2} + v_2(z_2, T) e^{ik_\mu z/2} \\ & + c_1^2 c_2^* v_3(T) e^{i(2-k_\mu)z/2} + c_1^* c_2^2 v_4(T) e^{-i(1-2k_\mu)z/2}. \end{aligned} \tag{5.9}$$

The first two terms in R_3 have the same fast-scale z -dependence as the lowest-order terms (5.3). It is well-known (see, e.g., Ref. 29) that in such a case coefficients v_1 and v_2 will grow linearly on the fast scale unless certain secular conditions are imposed on the amplitudes c_1, c_2 . These conditions are found using the method of Ref. 28,

$$i\alpha_1 \frac{dc_1}{dz_2} = \delta_{12} |c_2|^2 c_1, \tag{5.10}$$

$$i\alpha_2 \frac{dc_2}{dz_2} = (\delta_{21} |c_1|^2 + \delta_{22} |c_2|^2) c_2. \tag{5.11}$$

Here the parameters are

$$\alpha_1 = \int_{-\infty}^{\infty} \Phi_\mu^2 dT > 0, \quad \alpha_2 = \int_{-\infty}^{\infty} \Psi_\mu^2 dT > 0,$$

$$\begin{aligned} \delta_{12} = & - \int_{-\infty}^{\infty} dT [\Phi_\mu^2 f'_S [\Phi_\mu^2] (\Psi_\mu^2 + 2\Phi_\mu w_2) \\ & + \Phi_\mu \Psi_\mu f'_S [\Phi_\mu^2] (\Phi_\mu \Psi_\mu + 2\Phi_\mu w_3)], \end{aligned}$$

$$\delta_{21} = - \int_{-\infty}^{\infty} dT \Phi_\mu \Psi_\mu f'_S [\Phi_\mu^2] (\Phi_\mu \Psi_\mu + 2\Phi_\mu w_3^*),$$

$$\delta_{22} = - \int_{-\infty}^{\infty} dT \Psi_\mu^2 f'_S [\Phi_\mu^2] (\Psi_\mu^2 + 2\Phi_\mu w_2).$$

All coefficients α_j and δ_{ij} are real. Therefore, at order the distances $z \sim O(\nu^{-2})$, where $z_2 \sim O(1)$, Eqs. (5.10) and (5.11) describe self-consistent oscillations between the two orthogonal modes,

$$c_1 = C_1 e^{i\nu^2 \Delta k_1 z/2}, \quad c_2 = C_2 e^{i\nu^2 \Delta k_2 z/2}, \tag{5.12}$$

where C_1, C_2 are constant on the scale z_2 and

$$\Delta k_1 = -\frac{1}{\alpha_1} \delta_{12} |C_2|^2, \tag{5.13}$$

$$\Delta k_2 = -\frac{1}{\alpha_2} (\delta_{21} |C_1|^2 + \delta_{22} |C_2|^2).$$

Equations (5.12) are the main result of this section. They show that neither of the modes decays on the scale $z_2(O(\epsilon^{-1}\nu^{-2}))$. This is the key difference between the internal modes dynamics in the present model and that in the model considered in Ref. 28. The reason for the different behaviors of the two models is the following. The cross-terms (proportional to $c_1^*c_2$ and $c_1c_2^*$) in Eq. (5.4) have propagation constants, $\pm(1-k_\mu)/2$, that lie inside the gap of the continuous spectrum of the linear problem (3.7). Therefore, the corresponding terms, w_3 and w_4 , are both localized. On the contrary, for the model considered in Ref. 28, propagation constants of the cross-terms lie inside the continuous spectrum proper. Therefore, the counterparts of w_3 and w_4 for that case are not localized and describe radiation with a certain frequency generated away from the soliton. This radiation causes the higher-order internal mode to lose its energy exponentially fast. Such rapid (on the scale z_2) decay of that mode was confirmed by numerical simulations.²⁸

Now, similar considerations suggest that radiation-mediated decay of one of the localized modes can also take place in our model, but on a much longer scale. Indeed, the last term in expression (5.9) for R_3 has the propagation constant $-(1-2k_\mu)/2$ that lies inside the continuous spectrum of the linear problem (3.8). Therefore, the correction $v_4(T)$ is not localized in T and corresponds to radiation by the soliton at a certain frequency. This correction can be shown to be even in T ; thus the radiation is expected to have that parity and magnitude of order $O(\nu^3)$. However, such a weak radiation might only lead to very small effects which are definitely negligible for any practical situation and, moreover, whose resolution is beyond our numerical capability. To illustrate this, we simulate propagation of a background DM soliton with $S=0.5$ and the orthogonal component given by Eqs. (5.2), (5.3) with $\nu=0.13$ over 10 000 dispersion map periods. Other parameters in Eq. (1.1) are $\epsilon=0.2$ and $G(\xi)=1$. Our numerical simulations clearly show that both modes undergo small oscillations that do not decay visibly over 10 000 map periods. Figure 5 shows this for the odd internal mode; changes in both the amplitude and shape of the neutral mode are even smaller. Let us specifically note that the small ‘‘bumps’’ seen in Fig. 5(b) are not related to the radiation v_4 , because only the odd-parity part of the r -component is shown in that figure. Instead, those ‘‘bumps’’ are likely to be the result of the interaction between the weakly localized internal mode and the absorbing boundary used in our simulations.

To conclude this section, let us remark on existence of a stationary asymmetric soliton, mentioned in Sec. III. A limiting case of such a soliton would be the given by Eq. (3.3), with its r -component consisting of a single internal mode. If we repeat the analysis of this section while setting $c_1=0$, we do not find terms that can cause the soliton to radiate, at any

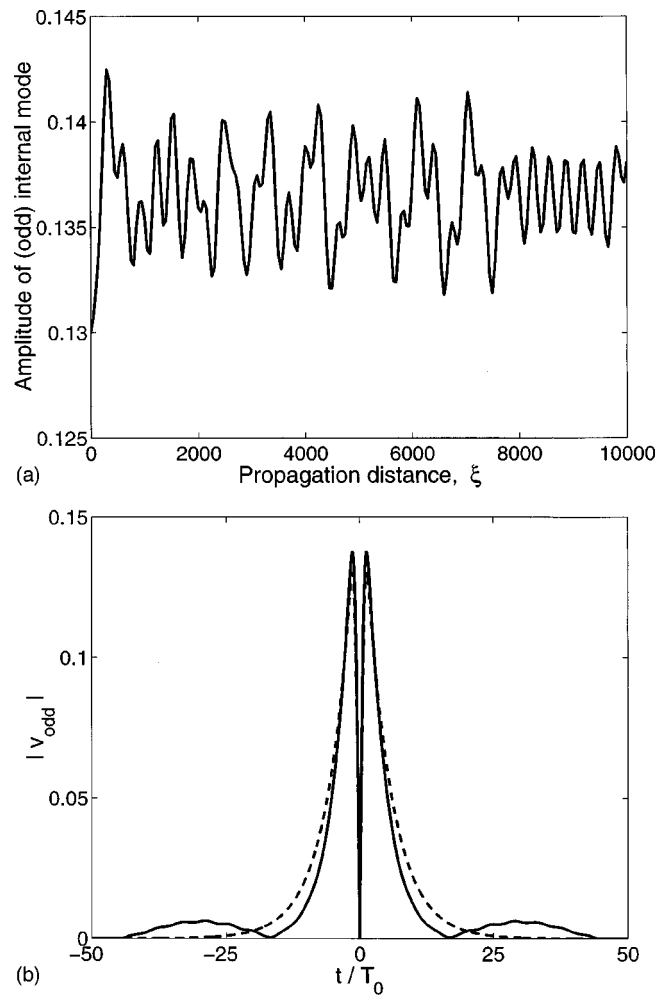


FIG. 5. (a) Evolution of the amplitude of the (odd) internal mode, recorded at every 50th map period. Other parameters are specified in Sec. V. (b) The initial (dashed line) and final (solid line) profiles of the same mode.

order in ν . This is a strong indication that a stationary asymmetric DM soliton indeed exists.

VI. CONCLUSION

In this work, we have demonstrated that both orthogonal and parallel internal (localized) modes exist on the background of a DM soliton. Our analysis was performed for the so called low-energy limit, where the nonlinearity and average dispersion affect the soliton evolution on a much longer scale than the local dispersion does. We found that the orthogonal modes exist for arbitrarily small map strength, whereas the parallel ones exist only when the map strength exceeds a certain threshold value. As the map strength approaches another critical value where the average dispersion changes its sign from positive to negative, the number of internal modes increases. Our numerical results suggest that for this critical value of the map strength, the number of both orthogonal and parallel internal modes is infinite. As one moves into the parameter region where the average dispersion is negative, these modes become quasilocalized, i.e., they develop oscillatory tails for $|t| \rightarrow \infty$. Yet, the numerical simulations demonstrate that if an initial perturbation to the exact DM soliton has a shape similar to that of a quasilocal-

ized mode near the soliton's central part, then the decay rate of such a perturbation into continuum radiation is very small.

We have also considered propagation of an orthogonal perturbation that consists of more than one internal mode. For the purpose of studying a long-term evolution, any generic perturbation can be thought of as consisting only of a finite number of internal modes, because the components of the continuous spectrum are "washed out" over shorter distances. We have shown that such a perturbation exhibits stable oscillatory dynamics over much greater distances than those required for telecommunication applications, with negligible amount of radiation being generated.

ACKNOWLEDGMENTS

The research of T.I.L. is supported by the National Science Foundation under Grant No. PHY94-15583. The research of D.E.P. is supported by the NSERC under NATO Postdoctoral Fellowship.

APPENDIX

In order to derive Eq. (2.13), we first substitute Eq. (1.3) into Eq. (2.2) and then use the formal Fourier transform of the Taylor expansion of $\exp[i\omega^2\Delta/2]$, similar to Eq. (2.6). As a result, we find

$$U = \langle u \rangle - \frac{iS}{2} \langle \Delta u \rangle_{TT} - \frac{S^2}{8} \langle \Delta^2 u \rangle_{TTTT} + O(S^3). \quad (\text{A1})$$

Here the angle brackets denote averaging over the map period. We have also used the scaling $t = T/\sqrt{S}$ [see Eq. (2.5)]. Next, we expand the solution of Eq. (1.1) for $D(\xi) = O(\epsilon)$ and $(S, \epsilon) \rightarrow 0$ in the asymptotic series as

$$u = \langle u \rangle + Su_1 + O(S^2), \quad (\text{A2})$$

where $\langle u_1 \rangle = 0$. Under the condition $h_1 = 0$, which we have assumed earlier, the form of u_1 becomes²²

$$u_1 = \frac{i}{2} \Delta \langle u \rangle_{TT}. \quad (\text{A3})$$

Finally, substituting Eqs. (A2) and (A3) into Eq. (A1) and using the definition of h_2 , found after Eq. (2.6), we arrive at Eq. (2.13).

- ¹N. J. Smith, N. J. Doran, W. Forysiak, and F. M. Knox, *J. Lightwave Technol.* **15**, 1808 (1997).
- ²S. K. Turitsyn, V. K. Mezentsev, and E. G. Shapiro, *Opt. Fiber Technol.: Mater., Devices Syst.* **4**, 384 (1998).
- ³T. I. Lakoba and D. J. Kaup, *Phys. Rev. E* **58**, 6728 (1998).
- ⁴D. E. Pelinovsky, Yu. S. Kivshar, and V. V. Afanasjev, *Physica D* **116**, 121 (1998).
- ⁵P. K. A. Wai and C. R. Menyuk, *J. Lightwave Technol.* **14**, 148 (1996).
- ⁶T. I. Lakoba and G. P. Agrawal, *J. Opt. Soc. Am. B* **16**, 1332 (1999).
- ⁷I. Gabitov and S. K. Turitsyn, *Opt. Lett.* **21**, 327 (1996).
- ⁸M. J. Ablowitz and G. Biondini, *Opt. Lett.* **23**, 1668 (1998).
- ⁹S. B. Medvedev and S. K. Turitsyn, *JETP Lett.* **69**, 499 (1999).
- ¹⁰J. H. B. Nijhof, N. J. Doran, W. Forysiak, and F. M. Knox, *Electron. Lett.* **33**, 1726 (1997).
- ¹¹N. J. Smith, N. J. Doran, F. M. Knox, and W. Forysiak, *Opt. Lett.* **21**, 1981 (1996).
- ¹²T. Yu, E. A. Golovchenko, A. N. Pilipetskii, and C. R. Menyuk, *Opt. Lett.* **22**, 793 (1997).
- ¹³S. K. Turitsyn and V. K. Mezentsev, *JETP Lett.* **67**, 640 (1998).
- ¹⁴S. V. Manakov, *Zh. Eksp. Teor. Fiz.* **65**, 505 (1973) [*Sov. Phys. JETP* **38**, 248 (1974)].
- ¹⁵V. S. Shchesnovich and E. V. Doktorov, *Phys. Rev. E* **55**, 7626 (1997).
- ¹⁶T. I. Lakoba and D. J. Kaup, *Phys. Rev. E* **56**, 6147 (1997).
- ¹⁷T. I. Lakoba, *Phys. Lett. A* **260**, 68 (1999).
- ¹⁸Yu. V. L'vov and I. R. Gabitov, "Dispersion management in optical fiber links: Integrability in leading nonlinear order," Los Alamos, preprint *chao-dyn/9907007*.
- ¹⁹Yu. S. Kivshar, D. E. Pelinovsky, T. Cretegnny, and M. Peyrard, *Phys. Rev. Lett.* **80**, 5032 (1998).
- ²⁰Y. Kodama and A. Maruta, *Opt. Lett.* **22**, 1692 (1997).
- ²¹A. Hasegawa and Y. Kodama, *Opt. Lett.* **16**, 1385 (1991).
- ²²T.-S. Yang and W. L. Kath, *Opt. Lett.* **22**, 985 (1997).
- ²³T. Kapitula, *Physica D* **116**, 95 (1998).
- ²⁴D. E. Pelinovsky, J. E. Sipe, and J. Yang, *Phys. Rev. E* **59**, 7250 (1999).
- ²⁵S. K. Turitsyn, *Phys. Rev. E* **58**, R1256 (1998).
- ²⁶C. T. H. Baker, *Numerical Solution of the Eigenvalue Problem*, in *Numerical Solution to Integral Equations*, edited by L. M. Delves and J. Walsh (Clarendon, Oxford, 1974), Chap. 10, p. 125.
- ²⁷D. J. Kaup, *Phys. Rev. A* **42**, 5689 (1990).
- ²⁸D. E. Pelinovsky and J. Yang, "Internal oscillations and radiation damping of vector solitons," *Stud. Appl. Math.* (to be published).
- ²⁹A. H. Nayfeh, *Introduction to Perturbation Techniques* (Wiley, New York, 1981), Sec. 4.5, p. 126.